INL/JOU-21-65213-Revision-0

Improving bamboos fuel and storage properties with a net energy export through torrefaction paired with catalytic oxidation

July 2022

Nepu Saha, Eric P Fillerup, Brad J Thomas, Corey David Pilgrim, Thomas P. Causer, Dan Herren, Jordan Lee Klinger

Changing the World's Energy Future

INL is a U.S. Department of Energy National Laboratory operated by Battelle Energy Alliance, LLC

INL/JOU-21-65213-Revision-0

Improving bamboos fuel and storage properties with a net energy export through torrefaction paired with catalytic oxidation

Nepu Saha, Eric P Fillerup, Brad J Thomas, Corey David Pilgrim, Thomas P. Causer, Dan Herren, Jordan Lee Klinger

July 2022

Idaho National Laboratory
Idaho Falls, Idaho 83415

http://www.inl.gov

Prepared for the
U.S. Department of Energy
Under DOE Idaho Operations Office
Contract DE-AC07-05ID14517, DE-AC07-05ID14517

Improving bamboo's fuel and storage properties with a net energy export through torrefaction paired with catalytic oxidation

Nepu Saha[a], Eric Fillerup[a], Brad Thomas[a], Corey Pilgrim[a], Thomas Causer[b], Dan Herren[b], and Jordan Klinger[a]*

[a]Idaho National Laboratory, 1955 N. Fremont Avenue, Idaho Falls, ID 83415, USA

[b]Advanced Torrefaction Systems, 439 South Kirkwood Road, Suite 204, Kirkwood, MO 63122, USA

* Corresponding Author: Email: jordan.klinger@inl.gov, Tel: +1 208 526 3528

Abstract

Using torrefied char, or biocoal, as solid fuel provides an opportunity to introduce a sustainable feedstock into the energy market. The goals of this study were to investigate how torrefaction improves the energy content and the grindability of a Malaysian bamboo along with understanding the potential for integrated energy recovery from torrefaction gases. The feedstock was torrefied at 250–290 °C for 1 h and the combustion characteristics and grindability of the solid products along with the composition of torrefied gas species were measured. The results showed a beneficial increase in elemental carbon increased from 47 to 63 wt% at 290 °C torrefaction, reflecting an increase in higher heating value from 17.8 to 25.6 MJ/kg. The combustion behavior of all the products showed three distinct zones, with increasing torrefaction severity leading to higher combustion temperature due to an increased fixed carbon content. This increase in severity also lead to more friable and grindable material, and the 290 °C condition required a factor of 2.7 less hold-up time in the mill compared to the raw bamboo, and a factor of 8.5 less energy (938 and 111 kWh/tonne respectively). Through analysis of the gas and volatile formation, a case study showed that catalytic oxidation can convert nearly 100% of the embodied chemical energy into usable thermal energy. These experimental findings were scaled to a 100,000 tonne/y capacity torrefaction plant and in the moderate case of 270 °C operating temperature, the plant has 1.25 GJ/tonne excess energy beyond what the process needs.

Keywords: torrefaction; catalytic oxidation, energy recovery, combustion characteristics; grinding energy.

Graphical Abstract:

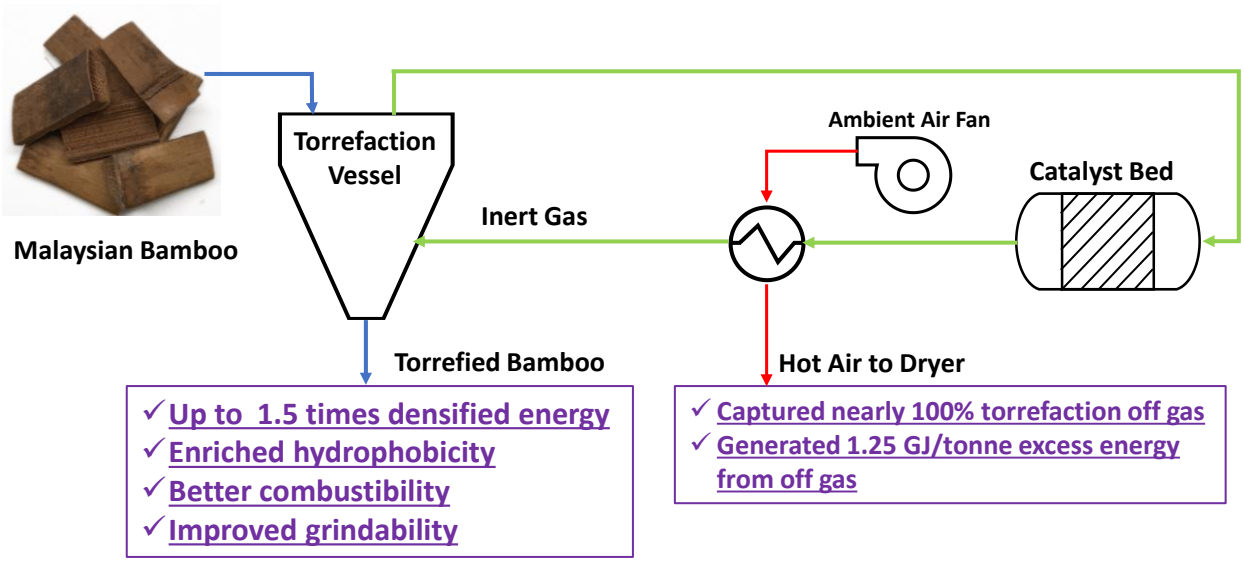

Highlights

- Torrefaction at higher temperatures positively enhances higher heating value.
- Grinding energy reduced 8.5 times with the increase of torrefaction temperature.
- Catalytic oxidation converts chemical energy in the volatiles into thermal energy.
- 1.25 GJ/tonne excess energy can be generated from torrefaction gas.

1 Introduction

In the past few decades, renewable energy sources have been getting more attention due to the desire to limit the use of fossil fuels amid increasing environmental concerns caused by climate change. Biomass is one of the dominant sources of renewable energy. According to the U.S. Energy Information Administration, biomass provided 39% of the total renewable energy consumed in the U.S. in the year 2020 [1]. Due to wide availability and the potential to achieve greenhouse gas neutrality, biomass has become a potential candidate for replacing fossil fuels [2, 3]. Biomass resources, usually used for fuel or energy, include energy crops, residues (e.g., forestry, agricultural crop, wood), wet wastes (e.g., food wastes, algae), and municipal wastes. In recent times, bamboo, a grassy lignocellulosic biomass, which is widely distributed in many countries across the world, has gotten the attention of many in the energy field. It is one of the fastest growing energy crops (matures within 5–7 y) [4] and occupies about 54,054 square miles of global land [5]. Even though a large supply of bamboo feedstock exists, due to the low calorific value and high hydrophilicity (tendency to adsorb moisture) in its raw form, it is less attractive as an energy source. To overcome those bottlenecks, various thermochemical conversions, such as torrefaction, hydrothermal carbonization, slow and fast pyrolysis, and gasification have been attempted [2, 4, 6-9]. Among those treatments, torrefaction is often seen as the most practical approach because torrefaction is usually conducted at comparatively low temperatures and it requires less energy input when compared to other treatments [10, 11].

Torrefaction is a mild thermochemical process where wet feedstock (usually <15% moisture) is treated at temperatures typically between 200–300 °C at atmospheric pressure for residence times typically between 15 min to 1 h under an inert atmosphere [12-14]. Due to the relatively low treatment temperature and relatively short residence time, torrefaction offers the ability to improve

the energy density, durability, and hydrophobicity of biomass feedstocks [15, 16], and becomes more attractive in industrial applications. During this treatment, feedstock undergoes mainly devolatilization and depolymerization reactions along with minor carbonization [17-19]. The main product of this treatment is a solid energy source, commonly known as torrefied char or biocoal. Biocoal typically retains 50–80% of the mass and up to 90% of the energy of the biomass feedstock, depending on the treatment condition [7, 8, 17, 20-22]. Meanwhile, the torrefaction process creates a large amount of various gases that are commonly referred to as 'torrefaction gas'. Torrefaction gas is made up of both condensable and non-condensable gases. The non-condensable gases include carbon monoxide and carbon dioxide. The condensable gases include water and several volatile organic compounds (VOCs), including acetic acid, formic acid, methanol, lactic acid, furfural, and hydroxy acetone. These VOCs are a direct result of the decomposition process and exist in a gaseous mixture with a majority water component making the mixture a relatively low heat content value fuel. For successful and commercially viable torrefaction to occur, two conditions must be met. First, torrefaction must be undertaken in an inert or near-inert environment containing little or no oxygen. Secondly, the chemical energy contained in the torrefaction gas must be efficiently converted into thermal energy for use throughout the torrefaction system. Catalytic oxidation enables extremely efficient oxidation of the VOCs and, in doing so, produces a catalyst flue gas stream of essentially inert gas comprised of carbon dioxide, nitrogen and super-heated steam. This stream of essentially inert gas is of sufficient volume to allow the entire torrefaction process to take place in an inert environment that is essential for a commercial-scale process to operate safely and reliably over long periods of time. Traditional forms of thermal combustion (e.g., use of a thermal oxidizer) cannot produce this essential inert gas.

In the past years, researchers have studied how the torrefaction treatment affects the physiochemical and combustion properties of bamboo. For instance, Li *et al.* [4] reported that the elemental carbon along with the lignin content of the bamboo increased with the severity of the torrefaction where the hemicellulose reduced significantly. They also reported that the water absorption capacity of torrefied char reduced about 54% which confirms the enhancement of hydrophobicity. Recently, Ma *et al.* [23] studied the migration of oxygen during bamboo torrefaction. They observed that the torrefaction of bamboo at 300 °C could remove about 28.5% of the oxygen resulting in a significant improvement in the heating value. This study also confirmed that the oxygen was mostly released as gaseous form (e.g., CO_2, H_2O, CO, and hydrocarbons) during the torrefaction at elevated temperature. The most recent study by Hu *et al.* [7] on bamboo torrefaction investigated the combustion kinetic of the torrefied char along with its physiochemical properties. The key finding of this study reveals that torrefaction reduced the activation energy which led to the transition of the combustion mechanism from nucleation to diffusion. The above studies clearly showed that the physiochemical properties, including the combustibility of the bamboo, can be improved significantly with torrefaction treatment. However, the heterogeneity of raw biomass, including bamboo, is a key problem with its use as a feedstock for co-firing with coal in an existing coal-fired power plant [20]. This heterogeneity can cause feedstock flow problems that severely limit the continuous, reliable operation of the plant. To avoid this limitation, the biomass feedstock must be ground before it is introduced into the power plant's boiler. However, studies have shown that the energy required to grind raw biomass is very high, ranging from 50 to 1900 kWh/tonne depending on the feedstock, grinding size, and the mill used for grinding [24-26]. For a comparison, the energy required to grind coal is between 7 to 36 kWh/tonne [27]. In a study conducted by Mani and Phanphanich [20], it was shown that the energy

required to grind pine chips can be reduced an order of magnitude (from 237.7 to 23.9 kWh/tonne) through torrefaction of the biomass at 300 °C. However, to the best of the authors' knowledge, no study has been conducted to show the degree to which torrefaction improves the grindability of bamboo and the overall heat and mass balance of an industrial scale torrefaction system.

Thus, the objectives of this study were to investigate the physiochemical properties, energy content, yield, hydrophobicity, and grindability (in terms of energy required) of the torrefied bamboo char. In addition, how the catalytic oxidation of torrefaction gas could improve the heat and mass balance of a commercial torrefaction system was also explored. To achieve those objectives, bamboo was torrefied at three different temperatures (250, 270, and 290 °C) for 1 h residence time. The changes in mass yields, heat content as measured as higher heating value, energy yield, and gaseous species were investigated. The compositional analysis was also conducted to identify the variations of the chemical components such as cellulose, hemicelluloses, and lignin. Hydrophobicity of the char was examined in terms of polarity index and the free-to-bound water ratio. Additionally, the energy required to grind the char was determined. Finally, an industrial scale model was conducted to investigate the benefit of catalytic oxidation of torrefaction gases on the overall heat and mass balance of the plant. The physiochemical properties, energy savings from enhanced grindability along with the energy recovery from the torrefaction gases can pave the way to industrial scale torrefaction of Malaysian bamboo.

2 Materials and Methods

2.1 Materials

Malaysian bamboo (*Gigantochloa Scortechinii*) was received from a commercial vendor, Advanced Torrefaction Systems, LLC (Kirkwood, MO). The sample was received as chips with an average length, weight, and height of 42.1 ± 2.3 mm, 19.3 ± 2.4 mm, and 6.3 ± 0.6 mm,

respectively. The moisture content of the sample was between 13–15 wt%. The sample was torrefied as received at various temperatures.

2.2 Experimental methods

Bamboo chips were torrefied in two different units, i) in a LECO Thermogravimetric Analyzer (TGA) 701 (St. Joseph, MI), and ii) in an SPX Blue M batch oven (Williamsport, PA), both under a nitrogen environment. The torrefaction was carried out at 250, 270, and 290 °C for 1 h. About 2 g (wet basis) of raw biomass was loaded in the TGA for a typical torrefaction experiment. The sample was heated at a heating rate of 15 °C/min. The sample was heated from 25 °C to 110 °C and held at 110 °C for 30 min to remove moisture, followed by a ramp to the target temperature (250 or 270 or 290 °C) and held at that temperature for an additional 1 h. As soon as the residence time of 1 h was over, the sample was allowed to cool down to the room temperature. Throughout the experiment, nitrogen was flowing at 10 L/min to avoid any unwanted combustion. A similar set of experiments was conducted in an oven with a larger sample batch of about 3700 g (wet basis) raw bamboo chips. All other parameters were kept similar to the previously discussed torrefaction experiment in the TGA. After completion of each torrefaction experiment, the torrefied char was collected and stored in a Ziplock bag for further analyses. The solid mass yield (MY) on the dry basis of a torrefaction experiment was calculated by using Eq. *(1)*.

$$MY(\%) = \frac{Mass\ of\ dried\ torrefied\ char}{Mass\ of\ dried\ feedstock} \times 100\% \qquad (1)$$

The samples investigated in this study are defined as T-X and O-X, where X indicates the torrefaction temperature, T and O depict that the char derived from TGA and oven, respectively. In addition, the feedstock is defined as Raw in the following sections.

2.3 Product characterization

2.3.1 Ultimate analysis

Ultimate analysis of the raw bamboo and torrefied char was carried out using the Elementar Vario EL cube (Ronkonhoma, NY) analyzer to determine elemental carbon, hydrogen, nitrogen, and sulfur content. The analyzer was calibrated with a certified Alfalfa standard. During the analysis, the sample was combusted at 1150 °C in ultra-high purity (UHP) oxygen at a flowrate of 38 mL/min along with UHP helium carrier gas at a flowrate of 230 mL/min. The gas was analyzed using a thermal conductivity detector (TCD) to determine the elemental carbon, hydrogen, and nitrogen, while an infrared (IR) detector was used to measure the sulfur content. Oxygen content was calculated separately by the difference method which is a common method used in various studies [28, 29]. Elemental analysis was measured in triplicate for each sample.

Furthermore, the polarity index, a ratio between elemental oxygen and carbon, was calculated by using the elemental analysis of the raw bamboo and torrefied chars.

2.3.2 Free-to-bound water ratio

Bamboo samples of differing torrefaction severity were analyzed using Time Domain Nuclear Magnetic Resonance (TD-NMR) spectroscopy to investigate proportions of bound and free water in the material through examination of the spin-spin (T_2) relaxation characteristics of the material. The samples were initially analyzed via TGA to provide information on the basal water content of the material. After this analysis, samples were partitioned into 10 mm flat-bottomed NMR tubes, capped, and initial T_2 measurement were performed using the Carr-Purcell Meiboom-Gill (CPMG) experiment. The details of this experiment can be found elsewhere [30, 31]. Moisture content of the samples were adjusted by adding 18 MΩ·cm water incrementally to the samples (basal, 10%, 15%, 20%, 25%, 30%, and 35% moisture content by mass). After each increment, the samples

were allowed to equilibrate overnight at 40 °C. This incubation also maintained the samples at the inner temperature of the instrument which allowed for quick changeover between samples during experimental runs. The instrument used in this study was a Bruker Minispec (Billerica, MA, USA), where the CPMG experiment was run with an echo time of 0.04 msec and a total of 32,000 echoes were collected for each sample. A total of 128 transients were measured with a 5 s relaxation delay between each transient. Experimental data curves were fit in two ways, i) simple two-term exponential decay, and ii) the CONTIN protocol. These methods are discussed in detailed in the Supplementary Information.

2.3.3 Compositional analysis

Compositional analysis of the torrefied char along with the raw bamboo was conducted according to the laboratory analytical procedures for standard biomass analysis developed by National Renewable Energy Laboratory (NREL) [32]. Briefly, the sample was first extracted by water and ethanol using an accelerated solvent extractor (ASE) 350 (Waltham, MA). To ensure adequate and consistent extraction, it was conducted three times with both water and ethanol. The water extracts and extracted solids were acid hydrolyzed with sulfuric acid to determine non-structural and structural sugar content, respectively. The hydrolyzed liquids were neutralized using calcium carbonate, filtered through a 0.2 μm nylon syringe filter, and analyzed for sugars. The non-neutralized liquids were filtered and analyzed for organic acids. Sugars and organic acids were analyzed via high performance liquid chromatography (HPLC) on an Aminex HPX-87P column (BioRad Laboratories, Hercules, CA). The acid soluble lignin was determined by measuring the absorbance at 320 nm via an ultraviolet-visible spectrophotometer (Varian Cary 50, Agilent, Santa Clara, CA). The measured absorbance was converted to the concentration of lignin by using the Beer's Law with an extinction coefficient of 30.

2.3.4 Chlorine analysis

Chlorine content of raw and torrefied bamboo samples was measured using a Vario EL Cube (Elementar Americas Inc, Ronkonkoma, NY). Samples were combusted at 1150 °C in 300 mL/min air using stearic acid 98% (Fischer Scientific, Waltham, MA) as a promoter. Water was removed from the gas using a desiccant bed, then hydrogen chloride content was measured using an electrochemical detector with a limit of detection of 500 ppb. Calibration was performed and the response factor determined using glycine HCl >99% (Fischer Scientific, Waltham, MA) over a range of 100–5000 ppm, the response factor is known to be directly proportional (linear) to chlorine content down to the limit of detection.

2.3.5 Proximate analysis

Proximate analysis was carried out in a LECO Thermogravimetric Analyzer 701 (St. Joseph, MI). American Society for Testing and Materials (ASTM) standard method (D 7582) was used to determine the volatile matter (VM), fixed carbon (FC), and ash content in the feedstock and torrefied chars [33]. In short, the sample was first heated from room temperature (about 25 °C) to 107 °C at 6 °C/min heating ramp and held at this temperature until a constant weight was reached. The mass loss during this time was considered as moisture content. The sample was further heated up to 950 °C at a ramp of 50 °C/min and kept isothermal for 9 min to make sure all VM was removed from the sample. During these steps, an inert atmosphere was maintained by flowing UHP grade nitrogen at 10 L/min. For the determination of ash content, the instrument was allowed to cool to 600 °C. At this point, oxygen was introduced (3.5 L/min) instead of nitrogen, and the temperature was ramped to 750 °C at 13 °C/min and held until a constant weight was reached for the sample. This remaining weight was considered as the ash content of the sample. The FC content was determined by subtracting VM and ash percentages from 100%. The measured values on a

dry basis were corrected based on a calibration curve built on coal standards provided by LECO. Proximate analysis was triplicated for each sample.

2.3.6 Combustion characteristics

The combustion characteristics were also measured using the LECO TGA 701. In this case, the experiments were performed under an oxidative environment, so instead of nitrogen, the air was introduced from the beginning of the experiment at a flowrate of 8.5 L/min. The sample was heated from room temperature to 900 °C at a heating rate of 5 °C/min. Given the design of the instrument, six replicates were run simultaneously to improve data resolution and provide sufficient data for statistical analysis. From the six sets of combustion data, the best fit derivative thermogram (DTG) was generated for each sample. The DTG curves for the respective samples were composited and a line of best fit was applied to represent the degradation as a continuum. Phenomenologically the DTG curves appear to have three distinct degradation zones (see Figure S3). These zones are hypothesized to be related to the moisture, combustion of the early volatilization, and then the more thermally stable carbon-rich structures. Assuming a series of three first order and Arrhenius behavior of the kinetics for these pseudo-reactions, parameters were fit to minimize the squared error of the prediction with the composite DTG curves. The root means square error (RMSE) of prediction for the DTG curves ranged from 0.2 to 0.5 wt%/min, or approximately 8–10% of the maximum degradation rate, indicating adequate data representation. From the fitted DTG, the ignition temperature (T_i) at which the fuel starts to burn, the burnout temperature (T_b) at which the fuel completes the burn, and the temperature at which the maximum DTG appeared were determined.

2.3.7 Higher heating value (HHV)

A LECO AC600 (St. Joseph, MI) isoperibolic system was used to determine the higher heating values (HHV) of the studied samples. A standard ASTM method (D 5865) was followed for the HHV measurement [34]. In short, samples were combusted in a combustion vessel in presence of 450 psi UHP grade oxygen. All the calculations were made based on the methods stated in D 5865. HHV of each sample was at least triplicated to ensure the statistical significance. From the measured heating values, dry ash free HHV (HHV_{daf}), energy yield (EY), and energy density (ED) were calculated by using Eqs. *(2)*, *(3)*, and *(4)*, respectively.

$$HHV_{daf} = \frac{HHV\ of\ the\ sample}{1 - fraction\ of\ dry\ ash\ into\ the\ smaple} \quad (2)$$

$$EY(\%) = MY(\%) \times \frac{HHV_{daf}\ of\ torrefied\ char}{HHV_{daf}\ of\ raw\ raw\ bamboo} \quad (3)$$

$$ED = \frac{HHV_{daf}\ of\ torrefied\ char}{HHV_{daf}\ of\ raw\ raw\ bamboo} \quad (4)$$

2.3.8 Grinding of raw bamboo and torrefied chars

The raw bamboo and torrefied chars were further milled by using Thomas Wiley Mill (Swedesboro, NJ), a lab-scale grinder. The mill is equipped with 4 stationary and 4 rotating knives. A motor spins the inner rotor where the speed of the rotor was 800 RPM. A screen with 6 mm circular perforations and a surface area of 135 cm^2 was mounted with the mill to control large particle retention. The power and mass logger of the instrument were connected to a computer to log the experimental data with a frequency of at least 2 Hz. During a typical experiment, a whole chip of raw bamboo or torrefied char was fed into the mill and ground completely before adding the next chip with the idea that a starve-fed mill chamber has the most direct correlation between

increased power draw and material fracture energy. These data were further used to calculate the grinding energy of each sample. Prior to running the mill with chips, an empty baseline test was conducted. This no-load power consumption was considered for the calculation of the grinding energy requirement for each sample.

2.3.9 Torrefaction gas analysis

Several experiments were also performed in a tube furnace paired with gas analysis to determine the partitioning between gas species during torrefaction of bamboo. For these tests, the tube furnace and a high purity quartz tube (25 mm diameter and 1 m length) were preheated to the target reaction temperature prior to sample introduction. A sweep gas of high purity nitrogen (approximately 1 L/min) was used to decrease the oxygen concentration below 0.3 wt% as measured by a digital oxygen sensor (OXYIQ-211-00, GE). The gas stream then passed through a coalescing filter (25-64-50CS, 99.99% capture efficiency at 0.01 μm, United Filtration Systems) made from bonded silicate resins in preparation for gas analysis. A digital flow meter (FMA-4312, Omega Engineering) and a gas analyzer measured the flow rate and concentrations of the permanent gases from the reactions. The gas species were measured by an electrochemical sensor for O_2, and a non-dispersive infrared (NDIR) detector for CO, CO_2, CH_4 and the total hydrocarbons (HC). Hydrogen was quantified with a Nova Analytical Systems (Nigra Falls, NY) TCD sensor (7905A). Gravimetric measurements yielded the solid and liquid product amounts. Volumetric flow rates from the digital gas flow meter and the gas composition from the analyzer were used to detail the gas evolution. These tests used a single, whole bamboo chips as received to be consistent with oven and TGA processing methods.

3 Results and Discussion

3.1 Physiochemical properties of torrefied char

A series of experiments was conducted to investigate the effect of torrefaction temperature on Malaysian bamboo. The physiochemical properties, such as MY (considered only the dry solid), proximate and ultimate analysis of the raw and treated bamboo in the oven and the TGA are shown in Figure 1, Figure 2, and Table 1, respectively. Before finalizing the studied torrefaction temperature band between 250–290 °C, a couple of experiments were conducted at lower temperature (i.e., 210 °C and 230 °C). The MY results showed less than 10 wt% mass loss which indicates a minimal degradation of bamboo occurred under those conditions (210 and 230 °C). As a result, this study has been conducted at higher temperature. The variation of the MY of the solid was observed with an increase of treatment temperature from 250 to 290 °C, the MY decreased from 81.6 to 57.5% and 83.1 to 61.8% while the experiments were conducted in the oven and TGA, respectively. Previous studies also observed a similar range of mass yield between 55–79% for bamboo feedstock [6, 35], while the woody biomass (e.g., *Eucalyptus grandis*) showed a higher yield of about 80–96% [36] under the same operating conditions. This result proves that bamboo is more reactive than woody biomass during the torrefaction treatment. A similar study was conducted by Chen and Kuo [37], while they used bamboo, willow, coconut shell, and ficus benjamina as feedstock. They observed that the bamboo was more reactive than others at mild torrefaction temperature due to having higher hemicellulose. The oven MY comparatively showed a lower value compared to the TGA at each operating temperature. This could happen due to the slightly higher operation temperature or temperature control compared to the actual set temperature in the oven. As the size of the oven was significantly bigger than the TGA, it was difficult to control the oven at absolute setpoint, although the yields were consistent and repeatable

(<1.4% relative deviation within experiments, and <1.3% between experiments) and fell within experimental error. The yields suggest that the oven was at a higher temperature compared to the set value (internal K-type thermocouples verified an offset of 3–7 °C variance) which could ultimately result in a less mass yield. To proof our hypothesis, a 300 °C torrefaction was conducted in TGA and compared this MY with the O-290. The MY result (52.9 %) at 300 °C in the TGA supporting our hypothesis the O-290 MY was between T-290 and T-300.

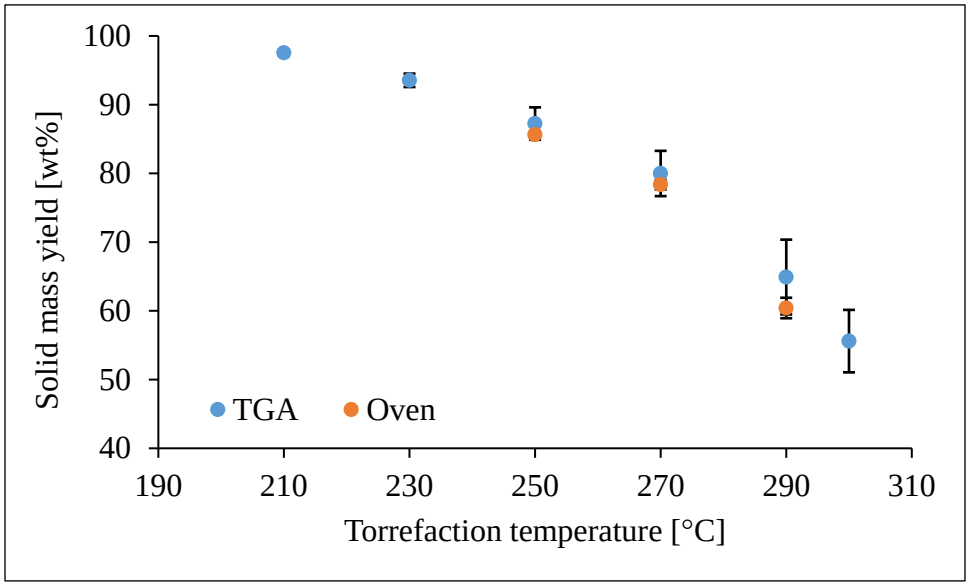

Figure 1: Solid yield of torrefied char. The blue marker indicates the TGA run, while the orange marker depicts the oven run. The solid yield decreases with the increase of torrefaction temperature.

It is clear from the previous paragraph that the mass yield decreases with the increase of torrefaction temperature which encourages the authors to further investigate the chemical properties (e.g., proximate, ultimate, etc.) of the torrefied char. The proximate analysis shown in Figure 2, indicates that the fixed carbon (FC) increased with the increase of temperature while volatile matter (VM) decreased. The FC and VM of the raw bamboo were observed about 15.0 ± 0.1 and 83.5 ± 0.0 wt%, respectively which was similar to the reported value in the literature [35]. With the increase of torrefaction temperature, FC showed an increasing trend while the VM exhibited a decreasing trend. For instance, FC and VM were 39.0 ± 0.1 wt% 58.0 ± 0.8 wt%,

respectively for the bamboo char produced at 290 °C. These results are in good agreement with the literature of woody biomass [38], which could happen due to the devolatilization reaction and/or thermal reticulation reactions [18, 19, 39]. An important reflection of the char was observed where the ash content increased with the increase of torrefaction temperature. For instance, the raw bamboo contains about 1.6 wt% ash where this value increased to about 3.0 wt% after torrefaction at 290 °C. However, the maximum observed ash number in this study (about 3.0 wt%) is still significantly lower than some coal standards (about 6.5–31.3 wt%) [40]. As the overall MY decreased with the temperature, the resulting increase of ash content was expected. J. S. Tumuluru [41] observes that the torrefaction does not do anything with the ash component of the biomass. He also noted that ash content is more relative to the original component of the biomass, as the volatiles and moisture content are mainly removed during the torrefaction, the ash content could relatively increase compared to the original feedstock. His claim was also supported by Chen *et al.* [42], where they mentioned that the volatile content of the biomass decreases during torrefaction resultant in an increase of the relative ash content in the torrefied char.

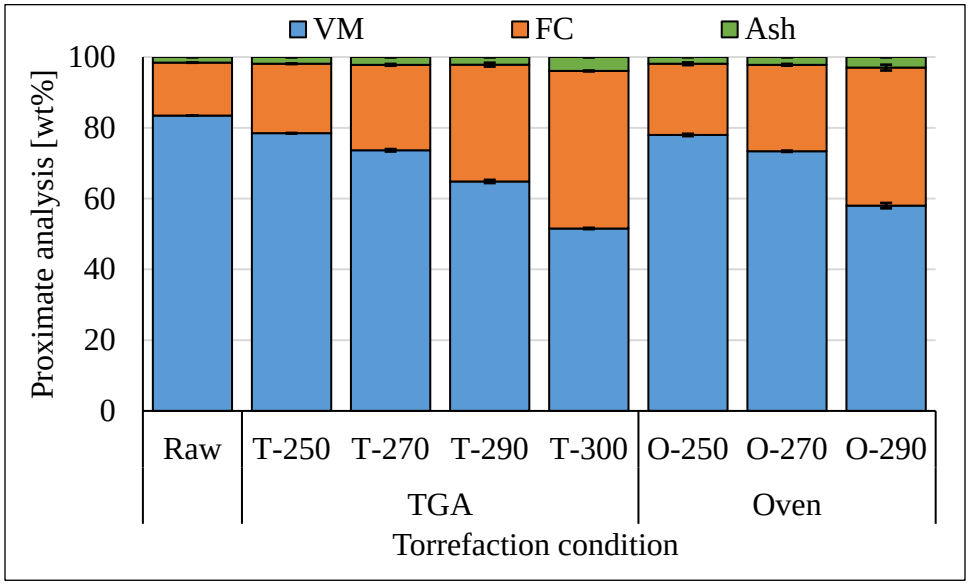

Figure 2: Proximate Analysis of torrefied char along with the raw bamboo. The blue, orange, and green stacks indicate the fixed carbon, volatile matters, and ash content, respectively. The fixed carbon increases with the torrefaction temperature while volatiles matter decreases.

The biomass mainly consists of five elements, such as carbon (C), hydrogen (H), oxygen (O), nitrogen (N), and sulfur (S), as well as some inorganics (usually referred to as ash). Elemental analysis of the studied samples was conducted and shown in Table 1. The measured nitrogen and sulfur contents were <0.6 and <0.1 wt%, respectively for all the samples. Both the nitrogen and sulfur contents were significantly low and there was no obvious trend with the torrefaction temperature. On the other hand, the carbon content of raw bamboo was 47.04 ± 0.11 wt% which increased about 35% to reach 63.37 ± 0.87 wt% at 290 °C during oven treatment. Consequently, the oxygen content reduced about 38% from its initial value of 44.83 ± 0.14 wt% to the final value of 27.81 ± 0.88 wt%. Although the hydrogen content showed a decreasing trend, however, this change was not severe compared to the change of carbon or oxygen. Increasing the carbon content while reducing the oxygen and hydrogen content with the severity of torrefaction temperature indicating that feedstock undergoes dehydration and decarboxylation reaction [43-45]. In the meantime, the polarity index, a ratio between oxygen and carbon content of the material, showed a decreasing trend (see Table 1). The decrease of polarity index with the increase of torrefaction temperature gives a hint that the surface is getting more hydrophobic with torrefaction severity [46]. In addition, it reveals the reduction of polar groups (−OH and C−O) occurred with the increase of torrefaction temperature [47]. To further investigate the hydrophobicity, the ability of the char to adsorb water was analyzed in terms of "free-to-bound water" using TD-NMR under different moisture levels (see Figure 3). Results showed that the increase of torrefaction temperature drives off excess water and volatile organic compounds while the chemical changes within the biopolymers in the bamboo occurred which allows the material to be more easily and homogenously ground down [48]. The loss of hydroxyl functional groups along the cell wall also

reduced the ability to adsorb water in the material [49], which further increased the fraction of free water in the sample. It can be seen in both analyses (Figure 3A and 4B) that the fiber saturation point is much higher for the low torrefaction samples [50], as a linear regime of increasing free water (which includes both free and bulk water in these analyses) appears at successively lower moisture content with increasing torrefaction temperature.

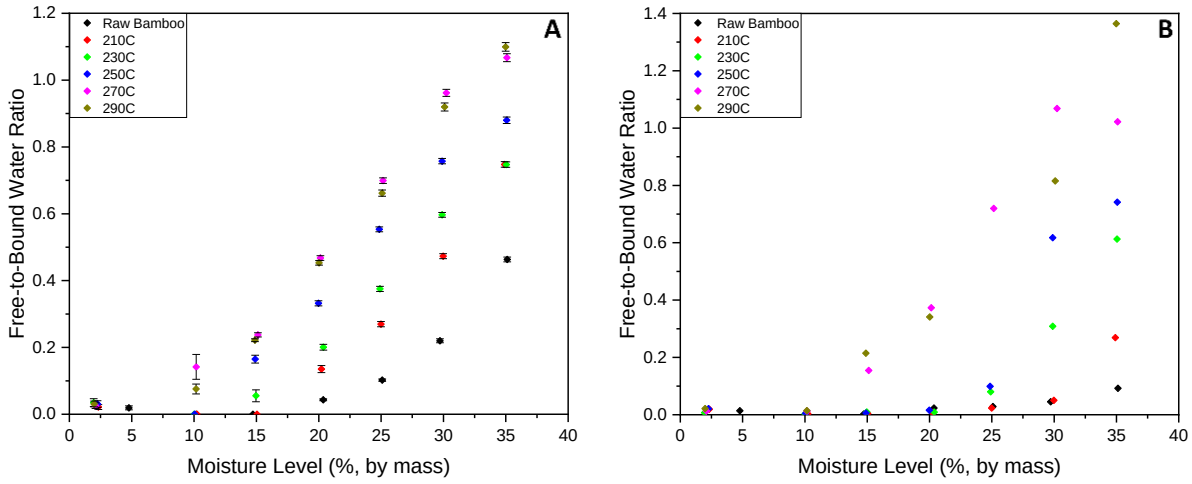

Figure 3: Free-to-bound water ratio as a function of moisture content in the torrefied bamboo samples. A) utilized the simple two-term exponential fitting routine, and B) utilized the CONTIN inverse Laplace transformation analysis.

To understand the reaction pathway during the torrefaction treatment, a van-Krevelen diagram which is a ratio between H/C and O/C was plotted and shown in Figure 4. Different dotted lines in the diagram indicate various reaction line pathways. For example, the orange lines indicate the dehydration reaction while the blue lines depict the decarboxylation reaction, and the gray lines describe the demethylation reaction. The material more towards the origin of the graph is considered a better fuel. Results showed that with the increase of the torrefaction temperature the fuel properties enhanced, and it moved from the biomass to the lignite and coal regions. It is also observed from Figure 4 that the bamboo undergoes mainly dehydration reaction along with marginally decarboxylation reaction. Due to the dehydration reaction, a decrease of O−C and H−C

bonds and an increase in the high energy C−C bonds could happen [6], resulting in an enhancement of the energy content of the torrefied char. To prove this hypothesis, we further investigated the higher heating values of the torrefied chars and compared them with the raw bamboo which is discussed in the following section 3.2.

Table 1: Ultimate and compositional analyses of torrefied char along with raw bamboo.

Sample	Ultimate Analysis (wt%)*					Total Chlorine (ppm)	Polarity Index	Compositional Analysis (wt%)*		
	C	H	N	S	O**			Hemicellulose	Cellulose	Lignin
Raw	47.04 ± 0.11	6.52 ± 0.02	0.03 ± 0.03	0.02 ± 0.00	44.83 ± 0.14	500 ± 470	0.71	16.18 ± 0.18	51.21 ± 0.14	28.1 ± 0.11
T-250	50.68 ± 0.02	6.11 ± 0.02	0.04 ± 0.06	0.02 ± 0.00	41.25 ± 0.09	530 ± 140	0.61	DNM***	DNM***	DNM***
T-270	53.40 ± 0.06	5.92 ± 0.01	0.08 ± 0.05	0.02 ± 0.00	38.39 ± 0.10	220 ± 70	0.54	DNM***	DNM***	DNM***
T-290	58.81 ± 0.20	5.51 ± 0.01	0.10 ± 0.04	0.02 ± 0.00	33.42 ± 0.23	120 ± 50	0.43	DNM***	DNM***	DNM***
T-300	66.86 ± 0.14	4.70 ± 0.18	0.61 ± 0.17	0.01 ± 0.00	23.88 ± 0.21	790 ± 270	0.27	DNM***	DNM***	DNM***
O-250	52.98 ± 0.09	5.94 ± 0.02	0.30 ± 0.01	0.08 ± 0.01	38.80 ± 0.13	210 ± 30	0.55	3.88 ± 0.03	48.78 ± 0.27	41.98 ± 0.8
O-270	54.84 ± 0.25	5.82 ± 0.04	0.35 ± 0.03	0.07 ± 0.00	36.72 ± 0.25	210 ± 90	0.50	1.42 ± 0.09	40.25 ± 1.21	53.87 ± 1.29
O-290	63.37 ± 0.87	5.40 ± 0.02	0.34 ± 0.03	0.09 ± 0.00	27.81 ± 0.88	150 ± 20	0.33	0.04 ± 0.01	17.88 ± 0.24	74.82 ± 2.35

* Dry basis, ** By the difference method, *** Did not measure

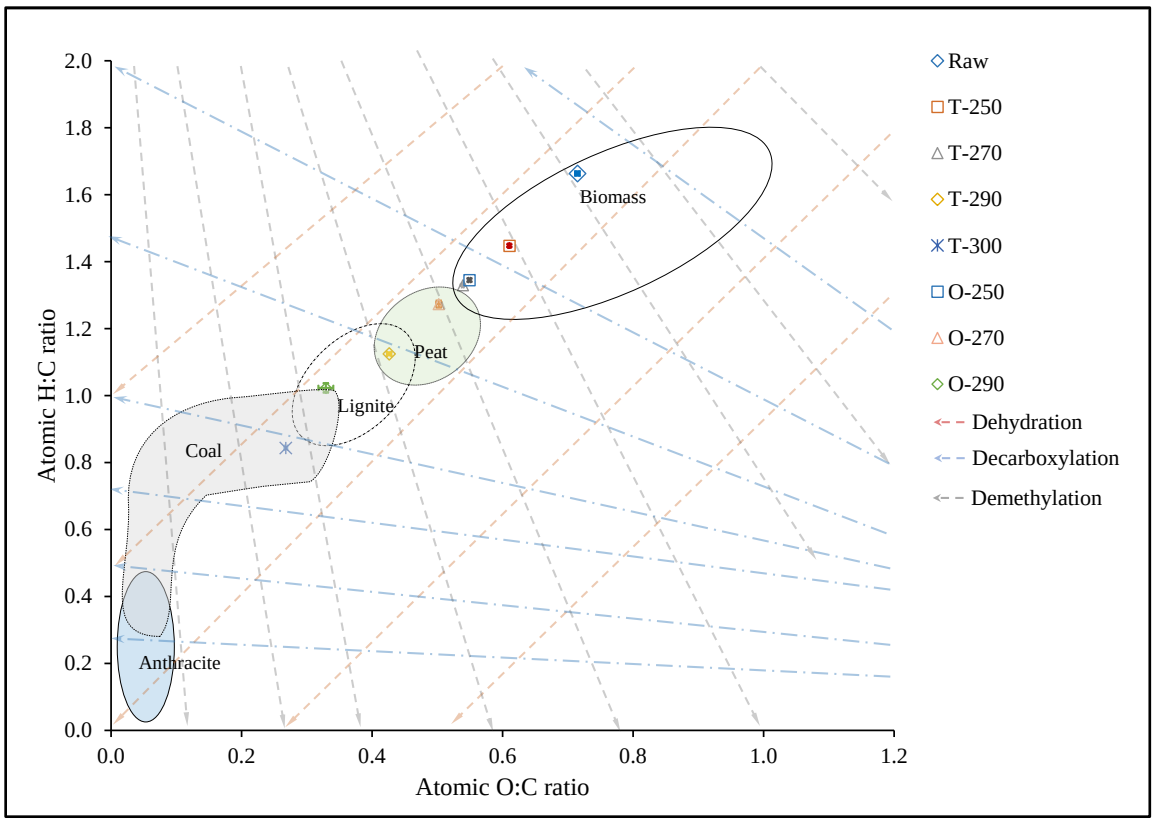

Figure 4: van-Krevelin diagram of the torrefied char. The bamboo moved towards the lignite and coal (sub-bituminous) reason with the increase of torrefaction temperature.

In addition to the physiochemical properties, visual inspection of the torrefied char showed that the bamboo turned into heavy black from light brown with the increase of torrefaction temperature (see Figure S1). This change in color indicates the formation of chromophoric group (e.g, C=O) which could form due to the structural change of lignin [51]. The compositional analysis shown in Table 1 furthermore confirms the significant increase of the lignin with the increase of torrefaction temperature. For instance, the lignin percentage increased from 28.1% to 74.8% for raw bamboo and O-290, respectively. Rousset *et al.* [8] reported a similar observation for bamboo where the lignin percentage increased from 27.0% to 68.7% at 280 °C torrefaction. Such a considerable increase of lignin concentration could occur due to either increase of insoluble matter (as carbohydrate degradation products) in acid solution [6] or the production of some lignin like products during the torrefaction which absorbs light at 320 nm (as per the lignin detection method)

or substantial loss of hemicellulose and cellulose components [8]. The elimination of polysaccharide cell walls during the torrefaction treatment could enhance the loss of hemicellulose components [8, 52].

Bamboo, like most plant matter, contains some concentration of chlorine. As the main product proposed in this work in a solid fuel, characterizing this is critical to ensure levels compatible with boiler configuration and maximum achievable control technology (MACT) where needed. This study further investigates the presence of chlorine in the raw bamboo and the torrefied chars (see Table 1). The chlorine content of the raw bamboo was measure about 500 ppm and generally showed a reducing trend with the increase of torrefaction temperature. Chlorine would undergo either migration and/or transformation to hydrogen chloride gas and tar during the torrefaction which could be the reason of having lower chlorine content in the torrefied char [53].

3.2 Energy content and density

The qualitative enhancement of fuel properties has already been observed from the van-Krevelen diagram discussed earlier (Figure 4). To quantify the energy content, we further measured the HHV_{daf} and calculated the EY and ED of the torrefied char which are shown in Figure 5. It can be observed from Figure 5 that the HHV_{daf} of the torrefied chars increased from 17.81 to 25.56 MJ/kg under the studied temperature. Similar to the previous findings, the oven derived char showed slightly higher HHV_{daf} compared to the TGA derived char at each corresponding temperature. The calorific values of the torrefied chars fall within the reported values of the lignite and sub-bituminous coal [54, 55]. The higher HHV signifies the improvement of ED as well. Figure 5 showed that the ED increased up to 1.44 times compared to the raw bamboo. Although both HHV_{daf} and ED increase, the EY decreases with the torrefaction temperature. As the EY closely related to the MY, this trend was expected. However, an important finding was observed where

the EY decreased only about 14% at 290 °C where the MY reduced about 40%. Since the heating value is positively correlated to carbonization/elemental carbon content [56], the higher HHVs support higher depletion of oxygen-rich carbohydrates, resulting in a higher degree of dehydration reactions during torrefaction which perfectly aligns with the van-Krevelen diagram (see Figure 4). In addition, a positive linear correlation (R^2 = 0.99) between the HHV_{daf} and the residual lignin was observed while the residual cellulose showed a negative linear correlation (R^2 = 0.93) (see Figure S2). These observations further confirm the increase of the calorific value of the torrefied char as the relative concentration of the residual lignin increases. From the EY, it was obvious that the torrefied char lost a portion of total energy content in the feedstock; however, fuel properties of the char could improve with the torrefaction treatment. To further investigate the fuel properties, a combustion characteristic of the torrefied char along with the raw bamboo was carried out and is discussed in the following section.

From the above discussion, it is clear that the trends of the physiochemical properties including the heating value of char produced in the oven and the TGA at a specific temperature are similar. However, the oven derived char at a specific temperature showed slightly advanced properties (e.g., high HHV, high carbon, low oxygen, etc.) compared to the TGA derived char at that temperature which could be due to a slightly higher operating temperature in the oven as discussed earlier. It was also understood that while the oven was set up at 250 °C, the actual operating temperature was between 250–270 °C, while the set temperatures were 270 and 290 °C, the true operating temperatures were between 270–290 °C, and 290–300 °C, respectively. As the properties discussed as of now for both oven and TGA derived char showed similar trends, the following sections will be proceeded only with the oven derived samples.

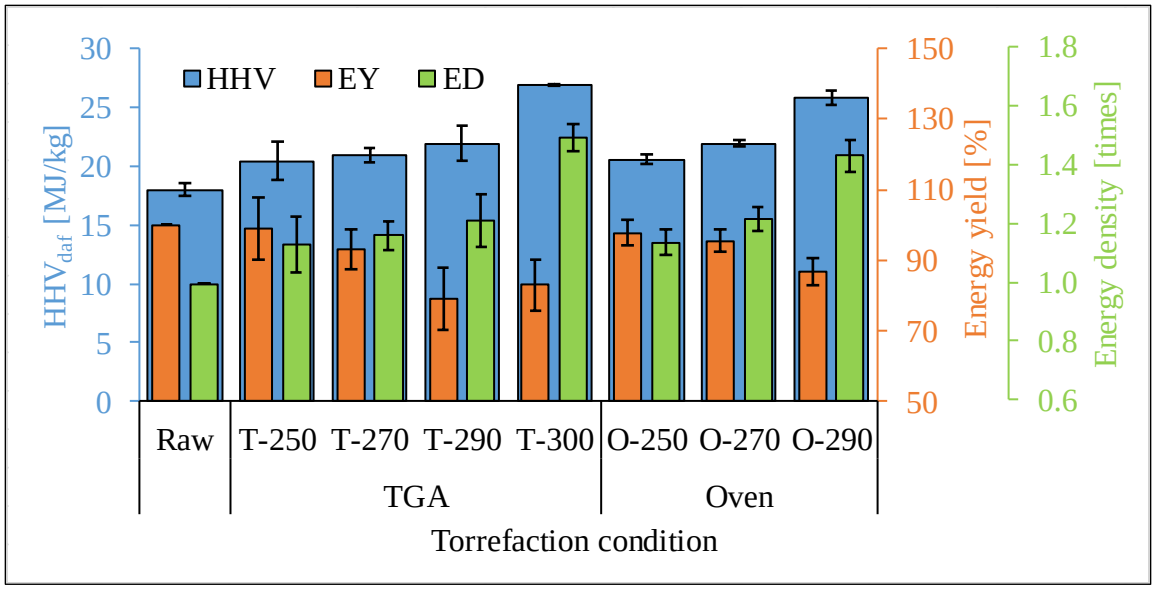

Figure 5: Dry ash free basis of higher heating value (HHV_{daf}) along with energy yield (EY) and energy density (ED) of bamboo and torrefied char. Although the EY decreased with the increase of torrefaction temperature, the HHV_{daf} and the ED showed an increasing trend.

3.3 Combustion characteristics

The experiments related to the combustion characteristics started with the whole chips of raw and torrefied bamboo. The whole chips showed very slow combustion and remained unburned even at 900 °C (see Figure S3). This could be due to the lower exposed surface resulting in lower heat transfer. While still a viable fuel source, they would only be practical for long residence-time combustors that could accommodate those dynamics. The same experiments were also conducted with ground samples (2 and 6 mm nominal retention sieve size). Interestingly, no significant change in the thermograms was observed between 2 and 6 mm samples, however, they were significantly different than the whole chips (see Figure S3). Although the materials were milled through 2 and 6 mm screens, the particle size distribution reflects that 50% of the particles were below 0.8 mm even when the materials were ground with a 6 mm screen (see Table S1). At the same time, 50% of the particles were below 0.4 mm when ground with a 2 mm screen. In both cases, the particle sizes were small enough to make a significant difference in the combustion behavior. For simplicity, the combustion behavior of a 6 mm ground sample is highlighted in the

main body here, and the remaining details are in the supplemental material. The D(TG) thermograms of the ground (6 mm) raw bamboo along with the torrefied bamboo are shown in Figure 6 which indicates a significant difference in the combustion behavior of the torrefied bamboo compared to the raw.

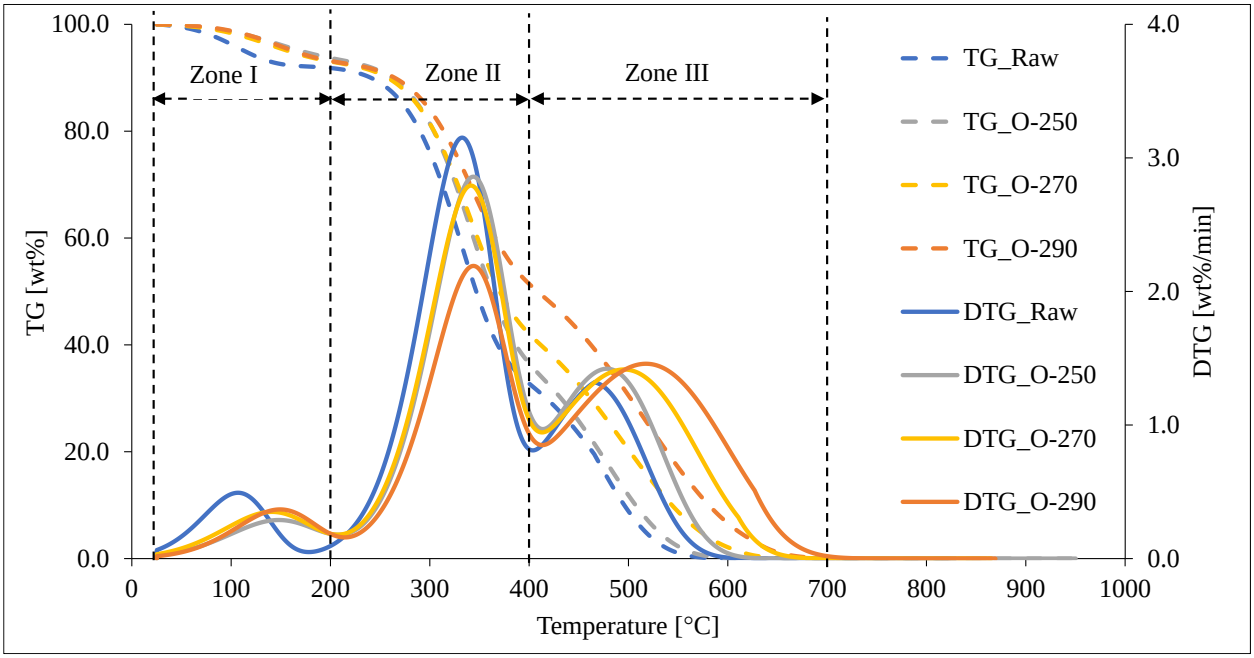

Figure 6: Fitted combustion TG and DTG curves for 6 mm grounded bamboo and their torrefied chars. Three different combustion zones were observed where the DTG curves shifted right to the temperature axis with the increase of torrefaction temperature.

The combustion behavior of all the studied samples appears to show three distinct combustion zones. It is hypothesized that Zone I (25–200 °C) is comprised mainly of moisture evaporation and/or the occurrence of extractives, Zone II (200–400 °C) is where the combustion of volatilization and decomposition of hemicellulose and cellulose occurred, and Zone III (400–700 °C) is where the combustion of fixed carbon and the residual lignin occurred. It is clear from Figure 6 that the most prominent rate of mass loss due to combustion occurred in Zone II and Zone III which accounted for more than 90% of total mass loss. Table 2 summarizes some of the combustion properties of raw bamboo along with the chars in Zone II and Zone III.

Table 2:Ignition and burnout temperature of raw bamboo and its torrefied chars along with the maximum rate of change in mass and the temperature at that maximum change.

Sample	Zone II				Zone III			
	T_i (°C)	T_b (°C)	DTG_{max} (wt%/min)	T @ DTG_{max} (°C)	T_i (°C)	T_b (°C)	DTG_{max} (wt%/min)	T @ DTG_{max} (°C)
Raw	210.60	390.20	3.15	332.60	405.80	560.15	1.32	465.75
O-250	240.60	400.40	2.86	343.80	420.60	580.20	1.42	478.40
O-270	235.80	396.40	2.79	341.40	420.20	630.60	1.42	495.60
O-290	240.40	398.80	2.19	344.00	420.20	675.75	1.46	517.60

In Zone II, no significant change in T_i and T_b was observed except compared to the raw bamboo. For example, the T_i and T_b for the raw bamboo were observed at about 210 and 390 °C, respectively, while for the chars, they were observed at between 235–240 °C and 396–400 °C, respectively. However, the DTG_{max} decreases with the increase of torrefaction temperature. The raw bamboo showed the maximum mass loss rate (3.15 wt%/min) while the O-290 showed the least rate loss (2.19 wt%/min) which could be due to the decreasing VM in the torrefied O-290 sample (see Figure 2). On the other hand, in Zone III, T_b shifted right on the x-axis which means an increasing behavior upon the increase of torrefaction temperature which is similar to the previously reported findings [7, 9], although the T_i showed a similar behavior as in Zone II. In Zone III, the DTG_{max} increases slowly with the torrefaction temperature while the temperature at DTG_{max} shifted right on the x-axis like the T_b. Shifting the T_b and temperature at DTG_{max} towards right on the x-axis indicates longer combustion times or temperatures are required and conclude that O-290 would be more thermally stable compared to raw bamboo and the less severe conditions. This, paired with a higher energy density, could provide a better fuel product to use in solid fuel boilers, as they would not undergo thermal decomposition during milling or pneumatic transport to the boiler with preheated/recycled air streams. Comparatively, this also relates to the highest and lowest presence of FC in the O-290 and raw sample, respectively. Furthermore, a relation between combustion properties (DTG_{max} and integral) and the proximate analysis was

developed to understand the combustion behavior which is shown in Figure 7. The VM showed a linear relation (R^2=0.99) with the DTG_{max} in Zone II while FC was poorly related (R^2=0.68) in Zone III which could be due to the presence of various forms of structural carbon, or more complex dynamics than those assumed here in this analysis. When the area under the curve (in Zone II and Zone III) were correlated with the VM and FC, a better linear relationship (R^2=0.88) was observed in Zone III which indicates that although the DTG_{max} at O-290 was not big enough to make the better linear relation with FC, the area under the curve (alternatively, the combustion zone) was big enough that further proof the longest combustion time of the O-290 among all the samples. Similar to the DTG_{max}, the area under the curve was also linearly correlated with the VM in Zone II (R^2=0.99).

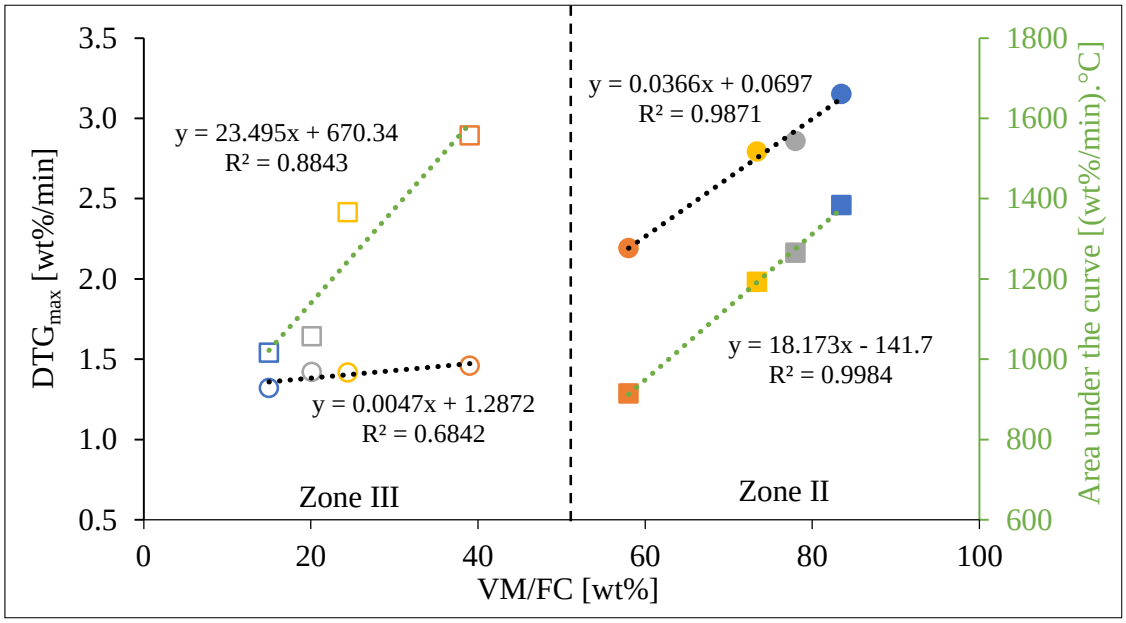

Figure 7: Correlation of VM and FC with DTG_{max} and area under the curve in Zone II and III. The hollow marker indicates the FC while the solid marker is for VM. The circle and square markers indicate the DTG_{max} and area under the curve, respectively. The blue, gray, yellow, and orange colors represent the raw bamboo, O-250, O-270, and O-290, respectively. Both DTG_{max} and the area under the curve linearly correlated with the VM in Zone II. Although, the area under the curve showed a linear relation with FC, but DTG_{max} showed a poor relationship in Zone III.

3.4 Grindability of torrefied char

As from the earlier discussion, we have seen that the fuel characteristics improve with the increase of the torrefaction temperature. It was also observed that the whole chips did not combust completely while the ground (reduced size) material did. Although size reduction is known as an energy intensive process, torrefaction has been shown to significantly reduce the hold-up time in mills as well as the energy required to fracture/fragment particles. The throughput and energy required for milling is shown in Figure 8. All the throughputs are normalized to 100% for comparison (sample sizes were consistent within ±5%). The throughput as a function of the feed mass is shown in the supplementary information (see Figure S4). It can be observed from Figure 8 that the time required to mill the raw bamboo is about 2.7 times higher than the torrefied bamboo. For example, it took about 5.5 s to grind 90% of the O-290 sample where about 15 s for the raw bamboo. As the throughput was significantly higher for torrefied char, the expectation was to have lower energy consumption compared to the raw bamboo which was exactly what was observed in this study and shown in Figure S5B. For instance, the energy requirement for raw bamboo grinding through a 6 mm screen was about 938 kWh/tonne where it was only 111 kWh/tonne for O-290. This is thought to be due to the torrefaction, as the volatile matters were reduced significantly which makes the sample more brittle [20, 27]. As a result, the torrefied char takes less energy to grind compared to the raw bamboo. Previously, the grinding energy of raw beech was reported about 850 kWh/tonne by Vincent *et al.* [27]. However, the grinding energy calculated for the raw bamboo in this study was still higher than the maximum reported value in the literature. This could be due to grinding a small amount of sample at a time in the mill. To proof this hypothesis, the authors increased the amount of feed (about 3–4 times more sample compared to the original load) in the mill and found that the energy required decreased about 18.2% and 9.2% for the raw bamboo

and the O-250, respectively (see Table S2). When the specific grinding energy is compared with the calorific value (HHV_{daf}), it can be observed that about 19.0% of the HHV_{daf} of raw bamboo is required just to grind it (see Figure 8). However, this percentage reduced significantly with the increase of torrefaction temperature and ended up only about 1.5% for O-290. As mentioned earlier, dehydration is the most dominant reaction that bamboo experienced during the torrefaction treatment which causes the shrinking of the feedstock [27]. As a result, some stress in the bamboo fibers could occur. At the same time, the shrinking could change the porosity of the materials. On the other hand, the thermal decomposition of bamboo could enhance the embrittlement of the cell wall. As a result of these consequences, the torrefied bamboo needs significantly less energy for grinding compared to the raw bamboo.

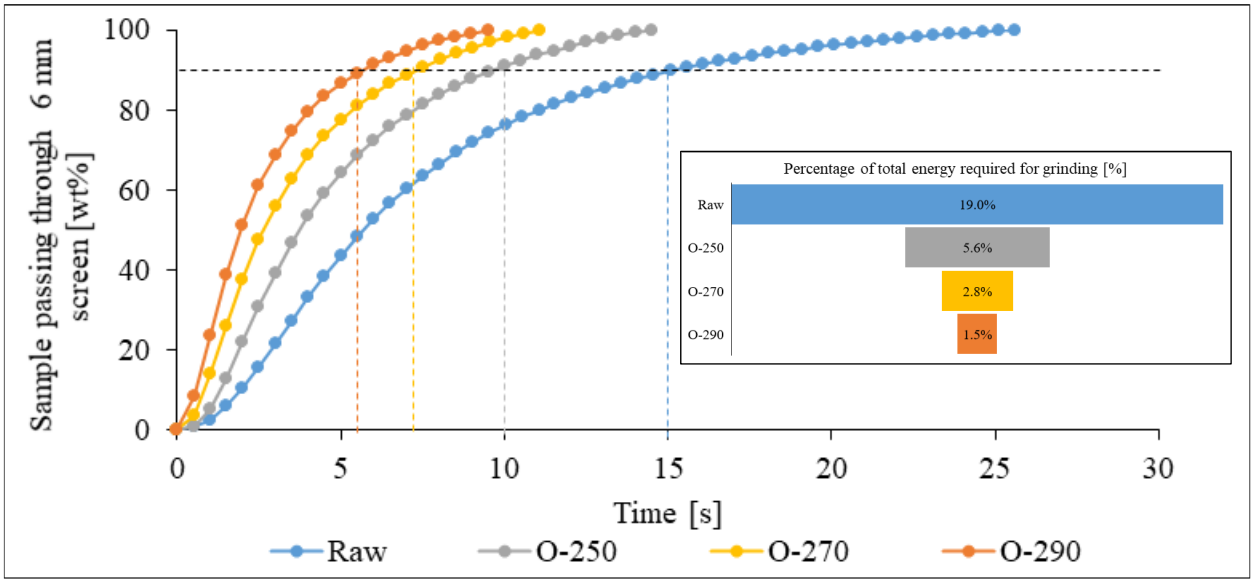

Figure 8: Time required to grind the raw bamboo along with the torrefied chars through 6 mm screen in a Wiley Mill with respect to the normalize mass. Percentage of energy required for grinding the char and raw bamboo corresponding to their own energy content (HHV_{daf}) is shown in as an overlap. Raw bamboo takes significantly high time consequently high percentage of energy for griding compared to the torrefied char.

It is clear from the above section that the torrefaction treatment significantly improves the grindability by reducing the time and energy required. At the same time a notable reduction of EY with the torrefaction severity was observed. This reduction of EY could challenge the grinding

benefit due to the torrefaction treatment. As torrefaction is a process which can be run auto-thermally, this could positively impact the overall energy balance. The following section will discuss the energy balance of a comprehensive system under various torrefaction temperatures to identify the overall significance of the torrefaction treatment.

3.5 Torrefaction off-gas analysis

As has been detailed earlier, torrefaction of bamboo changes its chemical composition. During the process of torrefaction, a minority portion of the raw bamboo solids volatilizes into a mixture of condensable gases (VOC liquids and water) and permanent gases. It has been shown that as the severity of the torrefaction operation increases, the torrefied solids increase in carbon concentration, decrease slightly in hydrogen content, and decrease significantly in oxygen content. The result is that the torrefied solids increase in heat content. The yields of both the permanent gases and the condensable gases increase with reaction temperature, and there is potential for energy recovery from both these organic vapors and permanent gases through combustion or thermal oxidation.

In addition to the torrefaction experiments reported earlier using a LECO thermogravimetric analyzer and a SPX Blue M batch oven, a tube furnace setup was used to detail and quantify the gases and condensable liquids produced during torrefaction of bamboo. The goal of this effort was to develop an understanding of the degree to which the chemical energy contained in these gases could be recovered, then converted to thermal energy via relatively low temperature catalytic oxidation, and subsequently used to sustain the torrefaction process operation. Prior work by our group has demonstrated that catalytic oxidation of the torrefaction gases is not only possible, but that catalytic oxidation is preferable to conventional thermal oxidation given the relatively high moisture content of these gases and the propensity of the torrefaction gases to form pyrolysis

liquids and tars [57]. Catalytic oxidation also provides an opportunity to produce an essentially inert catalyst flue gas capable of use in direct contact with the biomass during torrefaction and cooling operations. During the tests described above, 'as received' bamboo chips were inserted into the heated tube furnace to relate to 'as-received' industrial processing of the material. The bamboo decomposed and a mixture of resultant permanent gases and volatile liquids (plus water) were swept through a chilled condenser, a coalescing filter, and then to a gas analyzer for quantification of the off gases. Triplicate trials were performed at 250, 270 and 290 °C as presented in Table 3. Overall, the average solids yield agrees well with those obtained from the other methods described in detail above within experimental scatter.

Table 3. Gas analysis during torrefaction of bamboo at 250, 270, and 290°C.

Experimental Condition	Yield (%)			Gas Analysis (% of total gas)		
	Char	Liquid	Gas	CO	CO_2	HC
250, #1	83.89	13.98	2.13	4.87	85.18	9.95
250, #2	85.78	12.25	1.96	2.54	92.05	5.41
250, #3	86.86	10.90	2.24	2.37	85.72	11.91
250, Average	**85.51**	**12.38**	**2.11**	**3.26**	**87.65**	**9.09**
270, #1	83.11	12.63	4.26	3.88	87.91	8.21
270, #2	79.01	16.90	4.08	6.43	81.90	11.67
270, #3	79.06	16.08	4.86	5.21	85.28	9.50
270, Average	**80.39**	**15.20**	**4.40**	**5.17**	**85.03**	**9.79**
290, #1	68.07	28.67	3.26	9.47	75.44	15.05
290, #2	57.53	29.97	12.50	18.87	60.75	20.38
290, #3	66.07	29.04	4.89	11.33	70.80	17.84
290, Average	**63.89**	**29.23**	**6.88**	**13.22**	**69.00**	**17.76**

The changes in gas composition are also shown in Figure 9 as a function of dry solids yield. Although there is some scatter to the yield numbers tabulated above, they present a consistent trend when examined as a function of the degree of solids degradation. As the samples start to degrade, there is some formation of hydrocarbons (e.g., methane, ethane, etc.) and carbon monoxide, although the evolved gases are predominantly carbon dioxide, paired with the dehydration reactions discussed above resulting in the formation of reaction water. As the treatment increases in severity (from right to left in the Figure 9), the composition shifts toward a lower proportion of

carbon dioxide to higher concentrations of fuel gases. The lines in the plots are regression lines from quadratic fits to help illustrate/connect the discrete data measurements, rather than a known or assumed model. However, these non-linear trends in gas and vapor production are consistent with thermochemical conversion chemical kinetics models proposed in literature [58, 59].

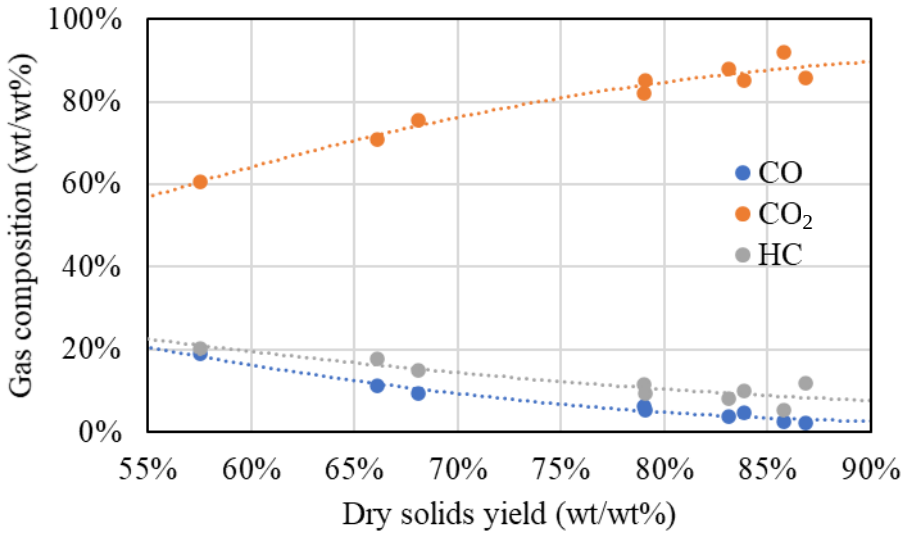

Figure 9. Gas yields from torrefaction with dry solids yield.

4 Torrefaction at Commercial Scale – An Example

Industrial deployment of torrefaction or any bioenergy technology requires careful consideration for plan performance, efficiency, and engineering exercises around mass balances and heat integration. To understand the viability of the currently studied biomass as a feedstock, it is instructive to consider the utilization of the data presented above and apply it to a commercial size torrefaction facility. To accomplish this, it is assumed in this illustrative example that the commercial torrefaction facility (operating at the moderate 270 °C condition) will have an annual production capacity of 100,000 tonne over 8,000 h of operation. A vertical mass flow reactor is simulated with an ATS Torrefaction Gas Treatment System utilizing ATS TorreCAT™ Catalytic Oxidation Technology. It is important to note that different torrefaction reactor designs can be

employed. For instance, rotary drums, rotary kilns, fluidized beds, and several other design approaches can be used with catalytic oxidation. A basic flow diagram for the process is shown in Figure 10. This reactor is charged from the top and the biomass proceeds down through the reactor. The hot, essentially inert catalyst flue gas at torrefaction temperature flows in a counter-current direction up through the biomass charged bed heating the biomass to torrefaction temperature, with volatile gases being generated as torrefaction occurs. Exiting the top of the reactor, the VOC laden gas stream is co-mingled with the evaporated water from the cooling operation, processed through a particulate removal system (cyclone separator), heated to an appropriate temperature, combined with pre-heated combustion air, and processed through an oxidation catalyst bed. A portion of the hot flue gas is used to indirectly heat the incoming VOC-laden stream and recombined with the balance of the flue gas. After removal of extra thermal energy via a heat exchanger with ambient air, most of the essentially inert gas is recycled back to the torrefaction reactor. Two minority slip streams are extracted from the majority stream prior to its return to the reactor. One slip stream is deemed to be more than the amount required to sustain torrefaction operations in the reactor. A second smaller slip stream is cooled and utilized in the cone of the reactor to begin the process of cooling the hot torrefied solids to a temperature where it is safe to remove.

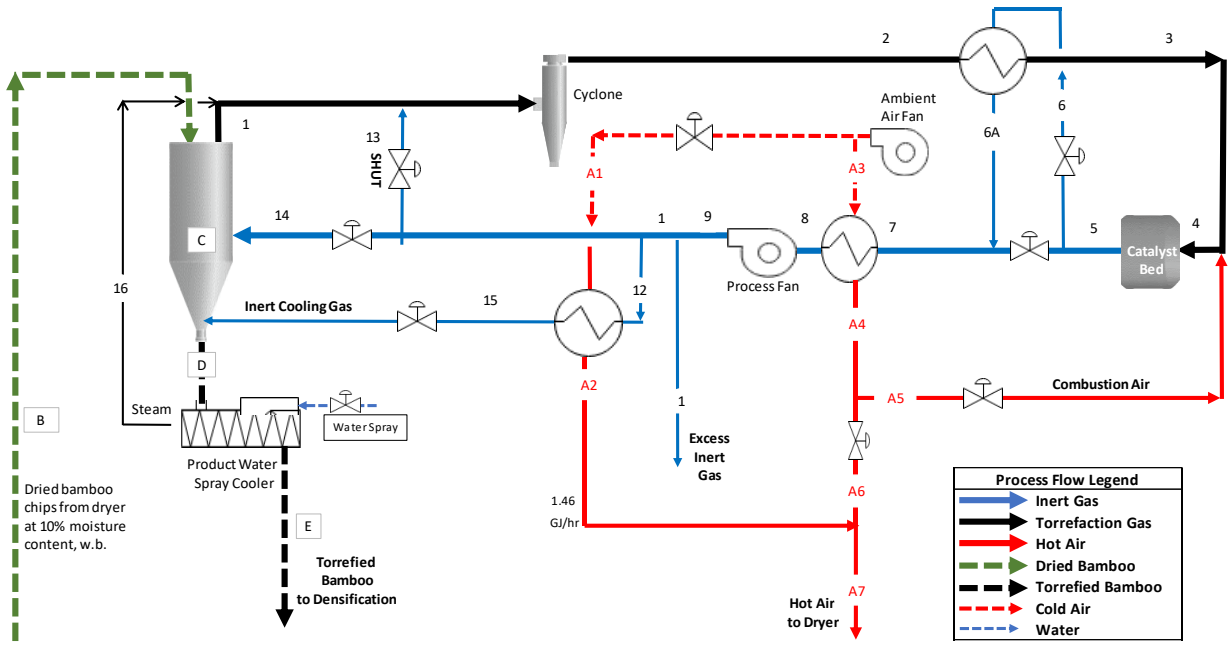

Figure 10: A basic process flow diagram of ATS torrefaction gas treatment system.

From data presented earlier in this study, a spreadsheet analysis for the elemental composition of the bamboo feedstock, torrefied bamboo solids, and the resulting off-gases are shown in Table 4. A breakdown of the process heat and mass balance for the system operating at 270 ºC is shown in Table 5. The descriptions of the gas streams are referenced by a stream number as illustrated in Figure 10. Similar to the solids, as the severity of torrefaction increases, so too does the amount of chemical energy store within the VOC laden gas phase products. Focusing on the intermediate case of 270 °C severity for processing, the yield of solid torrefied bamboo was 80.4% (solid/gas yield experiments above) and contained 2.220×10^6 GJ/y of the original 2.296×10^6 GJ/y embodied energy of the feedstock. Noting the significant concentration of oxygen (67.5%), mostly via the chemically formed water, the gases have a modest heating value of 2.76 MJ/kg, general composition of the torrefaction gases can then be calculated.

Table 4: Elemental composition of the bamboo feedstock, torrefied bamboo solids, and the resulting off-gases or a 100,000 tonne/y of a torrefaction facility. Note: the highlighted column is used as example in this study.

Material: Malaysian Bamboo									
Torrefaction Temperature, °C		**250**			**270**			**290**	
Solids Yield, %		**85.5%**			**80.4%**			**63.9%**	
FEEDSTOCK	Ultimate Analysis Results		tonne/y	Ultimate Analysis Results		tonne/y	Ultimate Analysis Results		tonne/y
	%C	47.1%	55,088	%C	47.1%	60,077	%C	47.1%	73,709
	%H	6.5%	7,602	%H	6.5%	8,291	%H	6.5%	10,172
	%O	46.4%	54,269	%O	46.4%	59,184	%O	46.4%	72,614
	%N	0.0%	-	%N	0.0%	-	%N	0.0%	-
	%S	0.0%	-	%S	0.0%	-	%S	0.0%	-
	%Ash	0.0%	-	%Ash	0.0%	-	%Ash	0.0%	-
	Total	**100.0%**	**116,959**	**Total**	**100.0%**	**127,551**	**Total**	**100.0%**	**156,495**
	Heat Content, HHV,MJ/kg		18.0	Heat Content, HHV,MJ/kg		18.0	Heat Content, HHV,MJ/kg		18.0
	Heat Content, GJ/y		2,105,263	Heat Content, GJ/y		2,295,920	Heat Content, GJ/y		2,816,904
TORREFIED BAMBOO	Ultimate Analysis Results		tonne/y	Ultimate Analysis Results		tonne/y	Ultimate Analysis Results		tonne/y
	%C	53.0%	53,000	%C	54.8%	54,800	%C	63.4%	63,400
	%H	5.9%	5,900	%H	5.8%	5,800	%H	5.4%	5,400
	%O	40.7%	40,700	%O	38.9%	38,900	%O	30.8%	30,800
	%N	0.3%	300	%N	0.4%	400	%N	0.3%	300
	%S	0.1%	100	%S	0.1%	100	%S	0.1%	100
	%Ash	0.0%	-	%Ash	0.0%	-	%Ash	0.0%	-
	Total	**100.0%**	**100,000**	**Total**	**100.0%**	**100,000**	**Total**	**100.0%**	**100,000**
	Torrefied Solids Yield		85.5%	Torrefied Solids Yield		80.4%	Torrefied Solids Yield		63.9%
	Heat Content, HHV, MJ/kg		20.5	Heat Content, HHV, MJ/kg		22.2	Heat Content, HHV, MJ/kg		25.8
	Heat Content, GJ/y		2,050,000	Heat Content, GJ/y		2,220,001	Heat Content, GJ/y		2,580,002
TORREFACTION GAS	Ultimate Analysis Results		tonne/y	Ultimate Analysis Results		tonne/y	Ultimate Analysis Results		tonne/y
	%C	20.5%	3,482	%C	24.1%	6,642	%C	24.9%	14,066
	%H	9.0%	1,527	%H	8.4%	2,324	%H	7.9%	4,489
	%O	70.5%	11,950	%O	67.5%	18,586	%O	67.2%	37,939
	%N	0.0%	-	%N	0.0%	-	%N	0.0%	-
	%S	0.0%	-	%S	0.0%	-	%S	0.0%	-
	%Ash	0.0%	-	%Ash	0.0%	-	%Ash	0.0%	-
	Total	**100.0%**	**16,959**	**Total**	**100.0%**	**27,551**	**Total**	**100.0%**	**56,495**
	Heat Content, GJ/y		55,263	Heat Content, GJ/y		75,918	Heat Content, GJ/y		236,902
	Heat Content, GJ/h		6.91	Heat Content, GJ/h		9.49	Heat Content, GJ/h		29.61
	Heat Content, MJ/kg		3.26	Heat Content, MJ/kg		2.76	Heat Content, MJ/kg		4.19

Calculated by difference

Table 5: Heat and mass balance of a 100,000 tonne/y torrefaction facility operating at 270 ºC.

Process Gas Streams									
Parameters	Torregas	1	2	3	4	5	6	6A	7
	Torrefaction Gases Generated	Torregas from Reactor	Torregas from cyclone	Torregas AFTER Process HE	Torrgas + Comb. Air into CAT	Torregas from CAT	Inert Gas into Process HE	Inert gas after Process HE	Hot Inert Gasa to H.E. #1
Mass, kg/h (1)	5,146	78,923	79,861	79,861	86,861	86,863	34,020	34,020	86,863
SCMM*	87	1,277	1,297	1,297	1,393	1,401	549	549	1,401
ACMM**	135	1,924	1,950	2,340	2,574	3,460	1,346	978	3,089
Temperature, °C	177	177	176	262	268	445	445	245	368
Wt% Volatiles (2)	26.81%	1.76%	1.74%	1.74%	1.60%	0.0%	0.0%	0.0%	0.0%
Vol% Volatiles (2)	11.90%	0.82%	0.80%	0.80%	0.75%	0.4%	0.4%	0.4%	0.4%

Process Gas Streams									
Parameters	8	9	10	11	12	13	14	15	16
	Inert gas from H.E. #1	Inert Gas from Process Fan	Excess Inert Gas	Inert Gas After Excess Inert gas	Inert Gas to H.E. #2	Dilution	Inert Gas to Reactor	Cooled Inert Gas into btm of reactor	Steam from Mixer Cooler
Mass, kg/h (1)	86,863	86,863	13,084	73,779	6,151	-	67,684	6,151	938
SCMM*	1,401	1,401	211	1,190	99	-	1,091	99	21
ACMM**	2,621	2,409	363	2,046	171	-	1,901	118	26
Temperature, °C	271	271	271	271	271	271	271	99	100
Wt% Volatiles (2)	0.0%	0.0%	0.02%	0.0%	0.0%	0.0%	0.0%	0.0%	trace
Vol% Volatiles (2)	0.4%	0.4%	0.4%	0.4%	0.4%	0.0%	0.4%	0.4%	trace

Air Flows							
Parameters	A1	A2	A3	A4	A5	A6	A7
	Ambient Air into H.E. #2	Heated Air FROM H.E. #2	Ambient Air into HE1	Heated Air FROM HE1	Combustion Air	Air 4 minus Combustion Air	Air 2 plus Air 6
Mass, kg/h	6,599	6,599	35,274	35,274	7,000	28,275	34,874
SCMM*	90	90	483	483	96	387	478
Temperature, °C	25	241	25	357	357	357	335

Solids Flow				
Parameters	B	C	D	E
	Bamboo into Torrefaction Reactor	Torrefied Bamboo at Reactor Gas Inlet	Torrefeid Bamboo exiting Reactor	Torrefied Bamboo exiting Water Cooler
Mass, kg/h	18,613	13,467	13,467	13,852
Water, kg/h	1,861	trace	trace	386
Wood, kg/h	16,751	13,467	13,467	13,467
Temperature, °C	25	270	200	80
% Moisture, w.b.	10%	0%	0%	3%

(1) Mass includes the free water from the feedstock entering the react

(2) Volatiles include carbon monoxide. Values showing 0.0% do contain trace amounts of VOC

* Standard cubic meter per minute

** Actual cubic meter per minute

The volatile mixture of gases generated during torrefaction has created both a challenge and an opportunity. As a challenge, these gases easily polymerize into liquids and tars. This then causes both safety and operational issues and becomes a roadblock to sustained commercial viability. By utilizing a catalytic oxidation system, these volatile gases are immediately oxidized and converted into a hot stream of inert gases consisting mainly of nitrogen, carbon dioxide, and steam. As an opportunity, these gases contain tremendous amounts of chemical energy. When converted via catalytic oxidation, the gases yield a large amount of thermal energy in the form of a hot, essentially inert, flue gas. Table 6 below illustrates the sources and uses of the energy contained in the torrefaction and catalytic oxidation system. From this analysis, the implementation of the thermal oxidation system enables the process to run without the need of external energy input. Further, 15.59 GJ/h (1.25 GJ/tonne product) is excess beyond what the process needs and is available for use in the drying function if the inert gas and hot air streams are combined. The use of catalytic oxidation allows for nearly 100% conversion of the chemical energy contained in the torrefaction gas into usable thermal energy in a manner that cannot be achieved with conventional thermal oxidation technology.

Table 6: The sources and uses of the energy contained in the torrefaction and catalytic oxidation system

Sources of Energy	**GJ/h**	**Contribution (%)**
Thermal energy released from the catalytic oxidation of the torrefaction gases	22.18	85.2
Thermal energy recovered during the operation of the torrefaction system	3.87	14.8
Total energy available	26.05	100
Uses of Energy	**GJ/h**	**Contribution (%)**
Net Torrefaction Reactor energy demand	9.69	37.2
Thermal energy exported as excess inert gas	4.41	16.9
Thermal energy exported as hot air to the drying function	11.18	42.9
Misc. energy losses	0.77	3.0
Total uses	26.05	100

This is a framework where bamboo was used as a feedstock, however, a similar outcome could be expected from other biomasses. A comprehensive investigation of how various biomasses

quantitatively track with these properties is planned for future work to draw more wider conclusions.

5 Conclusions

In its raw form, Malaysian bamboo is challenging to use in existing solid fuel-based power plants due to its low energy density and poor grindability. This study has presented how torrefaction treatment can improve both the energy content and the grindability of Malaysian bamboo. Additionally, this study presents the heat and mass balance including energy recovery from torrefaction gases via catalytic oxidation of a large-scale torrefaction facility. Bamboo was torrefied at various temperatures and the products were characterized in terms of ultimate and proximate analyses, compositional analysis, gaseous species analysis, TD-NMR, and energy content. The solid products were further investigated in terms of grindability and combustion characteristics while the gaseous products were used for potential energy recovery. The physiochemical properties of the char showed that the energy content increases significantly with the torrefaction severity. Similarly, the combustion characteristics also improved. The time and energy required to grind the torrefied char reduced significantly compared to the raw bamboo further proving the importance of the torrefaction. In addition, the large-scale demonstration showed that the torrefaction gases could be a significant energy source while converted via catalytic oxidation.

6 Acknowledgments

The research is supported by the U.S. Department of Energy (DOE), Office of Energy Efficiency and Renewable Energy (EERE), Bioenergy Technologies Office (BETO), under DOE Idaho Operations Office with Contract No. DE-AC07-05ID14517.

References

[1] U.S.E.I. Administration, U.S. primary energy consumption by energy source, 2020, Monthly Energy Review, 2021.
[2] W. Yan, S. Perez, K. Sheng, Upgrading fuel quality of moso bamboo via low temperature thermochemical treatments: Dry torrefaction and hydrothermal carbonization, Fuel 196 (2017) 473-480. https://doi.org/https://doi.org/10.1016/j.fuel.2017.02.015.
[3] Z. Liu, G. Han, Production of solid fuel biochar from waste biomass by low temperature pyrolysis, Fuel 158 (2015) 159-165.
[4] M.-F. Li, C.-Z. Chen, X. Li, Y. Shen, J. Bian, R.-C. Sun, Torrefaction of bamboo under nitrogen atmosphere: Influence of temperature and time on the structure and properties of the solid product, Fuel 161 (2015) 193-196.
[5] A.O. Oyedun, T. Gebreegziabher, C.W. Hui, Mechanism and modelling of bamboo pyrolysis, Fuel processing technology 106 (2013) 595-604.
[6] M.-F. Li, X. Li, J. Bian, C.-Z. Chen, Y.-T. Yu, R.-C. Sun, Effect of temperature and holding time on bamboo torrefaction, Biomass and Bioenergy 83 (2015) 366-372. https://doi.org/https://doi.org/10.1016/j.biombioe.2015.10.016.
[7] J. Hu, Y. Song, J. Liu, F. Evrendilek, M. Buyukada, Y. Yan, L. Li, Combustions of torrefaction-pretreated bamboo forest residues: Physicochemical properties, evolved gases, and kinetic mechanisms, Bioresource Technology 304 (2020) 122960. https://doi.org/https://doi.org/10.1016/j.biortech.2020.122960.
[8] P. Rousset, C. Aguiar, N. Labbé, J.-M. Commandré, Enhancing the combustible properties of bamboo by torrefaction, Bioresource Technology 102(17) (2011) 8225-8231.
[9] Z. Liu, W. Hu, Z. Jiang, B. Mi, B. Fei, Investigating combustion behaviors of bamboo, torrefied bamboo, coal and their respective blends by thermogravimetric analysis, Renewable Energy 87 (2016) 346-352. https://doi.org/https://doi.org/10.1016/j.renene.2015.10.039.
[10] B. Babinszki, E. Jakab, Z. Sebestyén, M. Blazsó, B. Berényi, J. Kumar, B.B. Krishna, T. Bhaskar, Z. Czégény, Comparison of hydrothermal carbonization and torrefaction of azolla biomass: Analysis of the solid products, Journal of Analytical and Applied Pyrolysis 149 (2020) 104844. https://doi.org/https://doi.org/10.1016/j.jaap.2020.104844.
[11] Q.-V. Bach, K.-Q. Tran, Ø. Skreiberg, R.A. Khalil, A.N. Phan, Effects of wet torrefaction on reactivity and kinetics of wood under air combustion conditions, Fuel 137 (2014) 375-383. https://doi.org/https://doi.org/10.1016/j.fuel.2014.08.011.
[12] M.J.C. van der Stelt, H. Gerhauser, J.H.A. Kiel, K.J. Ptasinski, Biomass upgrading by torrefaction for the production of biofuels: A review, Biomass and Bioenergy 35(9) (2011) 3748-3762. https://doi.org/https://doi.org/10.1016/j.biombioe.2011.06.023.
[13] M.J. Prins, K.J. Ptasinski, F.J.J.G. Janssen, More efficient biomass gasification via torrefaction, Energy 31(15) (2006) 3458-3470. https://doi.org/https://doi.org/10.1016/j.energy.2006.03.008.
[14] M. Atienza-Martínez, I. Fonts, J. Ábrego, J. Ceamanos, G. Gea, Sewage sludge torrefaction in a fluidized bed reactor, Chemical Engineering Journal 222 (2013) 534-545. https://doi.org/https://doi.org/10.1016/j.cej.2013.02.075.
[15] D. Thrän, J. Witt, K. Schaubach, J. Kiel, M. Carbo, J. Maier, C. Ndibe, J. Koppejan, E. Alakangas, S. Majer, F. Schipfer, Moving torrefaction towards market introduction – Technical improvements and economic-environmental assessment along the overall torrefaction supply

chain through the SECTOR project, Biomass and Bioenergy 89 (2016) 184-200. https://doi.org/https://doi.org/10.1016/j.biombioe.2016.03.004.
[16] P. Abelha, C. Mourão Vilela, P. Nanou, M. Carbo, A. Janssen, S. Leiser, Combustion improvements of upgraded biomass by washing and torrefaction, Fuel 253 (2019) 1018-1033. https://doi.org/https://doi.org/10.1016/j.fuel.2019.05.050.
[17] B. Acharya, I. Sule, A. Dutta, A review on advances of torrefaction technologies for biomass processing, Biomass Conversion and Biorefinery 2(4) (2012) 349-369. https://doi.org/10.1007/s13399-012-0058-y.
[18] W.-H. Chen, J. Peng, X.T. Bi, A state-of-the-art review of biomass torrefaction, densification and applications, Renewable and Sustainable Energy Reviews 44 (2015) 847-866. https://doi.org/https://doi.org/10.1016/j.rser.2014.12.039.
[19] S.-W. Park, C.-H. Jang, K.-R. Baek, J.-K. Yang, Torrefaction and low-temperature carbonization of woody biomass: Evaluation of fuel characteristics of the products, Energy 45(1) (2012) 676-685. https://doi.org/https://doi.org/10.1016/j.energy.2012.07.024.
[20] M. Phanphanich, S. Mani, Impact of torrefaction on the grindability and fuel characteristics of forest biomass, Bioresource technology 102(2) (2011) 1246-1253.
[21] S. Zhang, T. Chen, Y. Xiong, Q. Dong, Effects of wet torrefaction on the physicochemical properties and pyrolysis product properties of rice husk, Energy Conversion and Management 141 (2017) 403-409. https://doi.org/https://doi.org/10.1016/j.enconman.2016.10.002.
[22] D. Chen, A. Gao, K. Cen, J. Zhang, X. Cao, Z. Ma, Investigation of biomass torrefaction based on three major components: Hemicellulose, cellulose, and lignin, Energy Conversion and Management 169 (2018) 228-237. https://doi.org/https://doi.org/10.1016/j.enconman.2018.05.063.
[23] Z. Ma, Y. Zhang, Y. Shen, J. Wang, Y. Yang, W. Zhang, S. Wang, Oxygen migration characteristics during bamboo torrefaction process based on the properties of torrefied solid, gaseous, and liquid products, Biomass and Bioenergy 128 (2019) 105300. https://doi.org/https://doi.org/10.1016/j.biombioe.2019.105300.
[24] L.S. Esteban, J.E. Carrasco, Evaluation of different strategies for pulverization of forest biomasses, Powder Technology 166(3) (2006) 139-151. https://doi.org/https://doi.org/10.1016/j.powtec.2006.05.018.
[25] S. Mani, L.G. Tabil, S. Sokhansanj, Grinding performance and physical properties of wheat and barley straws, corn stover and switchgrass, Biomass and bioenergy 27(4) (2004) 339-352.
[26] M. Holtzapple, A. Humphrey, J. Taylor, Energy requirements for the size reduction of poplar and aspen wood, Biotechnology and Bioengineering 33(2) (1989) 207-210.
[27] V. Repellin, A. Govin, M. Rolland, R. Guyonnet, Energy requirement for fine grinding of torrefied wood, Biomass and Bioenergy 34(7) (2010) 923-930.
[28] M. Volpe, F.C. Luz, N. Saha, M.T. Reza, M.C.a. Mosonik, R. Volpe, A. Messineo, Enhancement of energy and combustion properties of hydrochar via citric acid catalysed secondary char production, Biomass Conversion and Biorefinery (2021). https://doi.org/10.1007/s13399-021-01816-z.
[29] D. Chen, A. Gao, Z. Ma, D. Fei, Y. Chang, C. Shen, In-depth study of rice husk torrefaction: Characterization of solid, liquid and gaseous products, oxygen migration and energy yield, Bioresource Technology 253 (2018) 148-153. https://doi.org/https://doi.org/10.1016/j.biortech.2018.01.009.
[30] S. Meiboom, Carr-Purcell-Meiboom-Gill sequence (CPMG), Rev Sci Instrum 29 (1959) 688-691.

[31] H.Y. Carr, E.M. Purcell, Effects of Diffusion on Free Precession in Nuclear Magnetic Resonance Experiments, Physical Review 94(3) (1954) 630-638. https://doi.org/10.1103/PhysRev.94.630.
[32] A. Sluiter, B. Hames, R. Ruiz, C. SCarlata, J. Sluiter, D. TempletOn, D. Crocker, Determination of structural carbohydrates and lignin in biomass, Laboratory analytical procedure 1617(1) (2008) 1-16.
[33] D. ASTM, 7582–12, Standard Test Methods for Proximate Analysis of Coal and Coke by Macro Thermogravimetric Analysis (2012).
[34] A. Standard, D5865-11A,“, Standard Test Method for Gross Calorific Value of Coal and Coke,” Appendix X 1 (2011).
[35] G. Sridhar, D. Subbukrishna, H. Sridhar, S. Dasappa, P. Paul, H. Mukunda, Torrefaction of bamboo, 15th European Biomass Conference Paper and Exhibition, Berlin, Gremany, 15th European Biomass Conference Paper and Exhibition, 2007, pp. 7-11.
[36] T.O. Rodrigues, P.L.A. Rousset, Effects of torrefaction on energy properties of Eucalyptus grandis wood, Cerne 15(4) (2015) 446-452.
[37] W.-H. Chen, P.-C. Kuo, A study on torrefaction of various biomass materials and its impact on lignocellulosic structure simulated by a thermogravimetry, Energy 35(6) (2010) 2580-2586. https://doi.org/https://doi.org/10.1016/j.energy.2010.02.054.
[38] B. Colin, J.L. Dirion, P. Arlabosse, S. Salvador, Quantification of the torrefaction effects on the grindability and the hygroscopicity of wood chips, Fuel 197 (2017) 232-239. https://doi.org/https://doi.org/10.1016/j.fuel.2017.02.028.
[39] M. Chaouch, M. Pétrissans, A. Pétrissans, P. Gérardin, Use of wood elemental composition to predict heat treatment intensity and decay resistance of different softwood and hardwood species, Polymer Degradation and Stability 95(12) (2010) 2255-2259. https://doi.org/https://doi.org/10.1016/j.polymdegradstab.2010.09.010.
[40] G.D. Mitchell, J.P. Mathews, Penn State’s Coal Repository: Penn State and Argonne Premium Coal Sample Bank & Database, International Conference on Coal Science & Technology, The Pennsylvania State University, PA, USA, 2013, pp. 1122-1132.
[41] J.S. Tumuluru, Comparison of Chemical Composition and Energy Property of Torrefied Switchgrass and Corn Stover, Frontiers in Energy Research 3(46) (2015). https://doi.org/10.3389/fenrg.2015.00046.
[42] D. Chen, J. Zhou, Q. Zhang, X. Zhu, Q. Lu, Upgrading of rice husk by torrefaction and its influence on the fuel properties, BioResources 9(4) (2014) 5893-5905.
[43] D. Chen, K. Cen, X. Cao, Y. Li, Y. Zhang, H. Ma, Restudy on torrefaction of corn stalk from the point of view of deoxygenation and decarbonization, Journal of Analytical and Applied Pyrolysis 135 (2018) 85-93. https://doi.org/https://doi.org/10.1016/j.jaap.2018.09.015.
[44] S. Zhang, T. Chen, W. Li, Q. Dong, Y. Xiong, Physicochemical properties and combustion behavior of duckweed during wet torrefaction, Bioresource Technology 218 (2016) 1157-1162. https://doi.org/https://doi.org/10.1016/j.biortech.2016.07.086.
[45] A. Sarvaramini, G.P. Assima, F. Larachi, Dry torrefaction of biomass – Torrefied products and torrefaction kinetics using the distributed activation energy model, Chemical Engineering Journal 229 (2013) 498-507. https://doi.org/https://doi.org/10.1016/j.cej.2013.06.056.
[46] N. Saha, D. Xin, P.C. Chiu, M.T. Reza, Effect of Pyrolysis Temperature on Acidic Oxygen-Containing Functional Groups and Electron Storage Capacities of Pyrolyzed Hydrochars, ACS Sustainable Chemistry & Engineering 7(9) (2019) 8387-8396. https://doi.org/10.1021/acssuschemeng.9b00024.

[47] Z. Chen, B. Chen, C.T. Chiou, Fast and slow rates of naphthalene sorption to biochars produced at different temperatures, Environmental Science & Technology 46(20) (2012) 11104-11111.
[48] T. Melkior, S. Jacob, G. Gerbaud, S. Hediger, L. Le Pape, L. Bonnefois, M. Bardet, NMR analysis of the transformation of wood constituents by torrefaction, Fuel 92(1) (2012) 271-280.
[49] J. Li, E. Ma, Characterization of Water in Wood by Time-Domain Nuclear Magnetic Resonance Spectroscopy (TD-NMR): A Review, Forests 12(7) (2021) 886.
[50] M.F. Froix, R. Nelson, The interaction of water with cellulose from nuclear magnetic resonance relaxation times, Macromolecules 8(6) (1975) 726-730.
[51] M.M. González-Peña, M.D.C. Hale, Colour in thermally modified wood of beech, Norway spruce and Scots pine. Part 1: Colour evolution and colour changes, Holzforschung 63(4) (2009) 385-393. https://doi.org/10.1515/HF.2009.078.
[52] P. Rousset, C. Lapierre, B. Pollet, W. Quirino, P. Perre, Effect of severe thermal treatment on spruce and beech wood lignins, Annals of Forest Science 66(1) (2009) 1.
[53] B. Peng, X. Li, J. Luo, X. Yu, Fate of Chlorine in Rice Straw under Different Pyrolysis Temperatures, Energy & Fuels 33(9) (2019) 9272-9279. https://doi.org/10.1021/acs.energyfuels.9b02097.
[54] O.C. Kopp, Subbituminous coal, Encyclopedia Britannica, 2019, pp. https://www.britannica.com/science/subbituminous-coal.
[55] P. Grammelis, N. Margaritis, E. Karampinis, 2 - Solid fuel types for energy generation: Coal and fossil carbon-derivative solid fuels, in: J. Oakey (Ed.), Fuel Flexible Energy Generation, Woodhead Publishing, Boston, 2016, pp. 29-58. https://doi.org/https://doi.org/10.1016/B978-1-78242-378-2.00002-X.
[56] M. Śliz, M. Wilk, A comprehensive investigation of hydrothermal carbonization: Energy potential of hydrochar derived from Virginia mallow, Renewable Energy 156 (2020) 942-950. https://doi.org/https://doi.org/10.1016/j.renene.2020.04.124.
[57] T. Westover, R.M. Emerson, Tests to Reduce TorreCat™ Technology to Practice, Idaho National Lab.(INL), Idaho Falls, ID (United States), 2016.
[58] J. Klinger, E. Bar-Ziv, D. Shonnard, T. Westover, R. Emerson, Predicting properties of gas and solid streams by intrinsic kinetics of fast pyrolysis of wood, Energy & Fuels 30(1) (2016) 318-325.
[59] J. Klinger, E. Bar-Ziv, D. Shonnard, Unified kinetic model for torrefaction–pyrolysis, Fuel Processing Technology 138 (2015) 175-183.